International Journal of Thermal Sciences 120 (2017) 244–251

Contents lists available at ScienceDirect

International Journal of Thermal Sciences

journal homepage: www.elsevier.com/locate/ijts

Characteristics of static pre-cyclonic steam ejector

Shengyang Tao, Yuqiang Dai*, Jiupeng Zou, Ding Zhao

School of Chemical Machinery, Dalian University of Technology, Dalian, 116024, China

ARTICLE INFO

Article history:
Received 1 November 2016
Received in revised form
3 May 2017
Accepted 14 June 2017

Keywords:
Steam ejector
Entrainment ratio
Supercharging ratio
Static pre-cyclonic steam ejector

ABSTRACT

The thermal vapor recompression (TVR) technology can partially recover condensation latent heat of the secondary steam in the multi-effect evaporation (MEE) process. And the two-dimension of x and r momentum exchange in the key device-steam ejector, makes induction efficiency relatively low and mixing length long. In this article, a novel three-dimensional momentum exchanging ejector called static pre-cyclonic steam ejector (SCSE) is first proposed. Its performances are mainly evaluated by means of computational fluid dynamics(CFD) at different dynamic pressure ratios (*DPRs*) and preliminarily validated by experiments. The SCSE can not only reduce the axial dimension of conventional ejector, but also show excellent performance at a low boosted pressure occasions. The SCSE with $DPR = 4/1$ improves the entrainment ratio(*ER*) by 10.8% compared to traditional ejector. For cases with secondary flow pressure disturbances, the application of the SCSE is limited because of an adverse impact on the operation stability. For cases with outlet flow fluctuates, the SCSE with larger *DPR* has higher peak *ER* and narrower choked-band-width at respective break-down supercharging ratios (*BSRs*), and there are no obvious influences on the operation stability for SCSE.

1. Introduction

How to deal with the high-salt wastewater has been a hot issue in the current academic research, and we urgently need cost-effective technology for its treatment [1,2]. Thermal desalination for high salinity wastewater treatments is one of the effective technologies nowadays, and has the prominent advantage of high desalination efficiency. As a supercharger in thermal vapor recompression technology[3], the steam ejector has the advantages of no moving parts, easy operation and maintenance, and low cost, etc. It can utilize part of latent heat of the secondary steam to save energy, and the energy-saving effect depends on its supercharging and entrainment characteristics. However, the shortcomings of low entrainment ratio (*ER*) and long-size mixture section limit the energy saving ability. Therefore, it has been a hotspot for a majority of researchers[4-6]to improve its performances.

Conventional ejector has a uniform structure. Its optimization process was to optimize the structure sizes of the primary flow [7,8] and mixing sections [9,10]so as to match the process conditions appropriately. X. Yang [11] tried some non-circle nozzles (such as oval nozzle, cross nozzle, rectangle nozzle, square nozzle et al.) of the driving primary stream, hoping to mix it more thoroughly with the secondary stream and improve the *ER*. Chang Y J [12] used a petal nozzle as the supersonic outlet of the primary flow. The breakdown pressure(BP) was about 22.3% higher than that of conventional nozzles, but the *ER* remained almost unchanged. Actually, all the above researchers tried their best to exchange the momentum of primary flow and secondary flow in axial direction. This study proposed a three-dimensional momentum exchange mechanism by introducing the cyclonical flow to the driving nozzle [13]or to the mixture section [14-15]. A novel prepositioned static pre-cyclonic steam ejector (SCSE)was developed and its supercharging characteristics were studied in detail.

2. SCSE's working principle and structure

2.1. SCSE's working principle

As shown in Fig. 1, the traditional ejector is mainly composed of primary nozzle, entrainment section, momentum exchanging section (or mixing section) and the supercharging section. Unlike the dynamic cyclonic steam ejector(DCSE) [16]which uses the high-speed rotating pseudo-blades placed in mixing section, the proposed SCSE has no moving parts, and uses a cyclone-generation module either placed at upstream of the primary nozzle or at

* Corresponding author. School of Chemical Machinery, Dalian University of Technology, Dalian, Linggong Road No.2, 116024, China.
E-mail address: daiyuqiang@dlut.edu.cn (Y. Dai).

http://dx.doi.org/10.1016/j.ijthermalsci.2017.06.009
1290-0729/

Nomenclature

Alphabetics

A	amplitude
BSR	break-down supercharging ratio
DPR	dynamic pressure ratio
L	length of the constant section in mixing chamber
Lc	distance between the main nozzle outlet and inlet of the mixing chamber
m	mass flux (kg s^{-1})
R	radius of mixing chamber
T	temperature(K)
APP	axial partial pressure
CSR	critical supercharging ratio
ER	entrainment ratio
P	pressure (Pa)
SR	supercharging ratio
TPP	tangent partial pressure

Greeks

ω	frequency (Hz)
θ	Diverging angle

Subscripts

t	total
s	secondary flow
h	high
i	primary flow
o	the outlet flow
l	low

downstream (like a chevron module) to divide the dynamic pressure into axial part and circumferential part of the driving stream. These two types of SCSEs are called prepositioned SCSE and post-positioned SCSE respectively.

In the primary driving flow, when the high pressure saturated steam passes through the cyclone-generation module, the tangential momentum will be generated besides the axial momentum. When flowing through the primary nozzle, the driving steam accelerates up to the sound speed and then supersonic speed with a very low pressure at the outlet, and finally jets into the

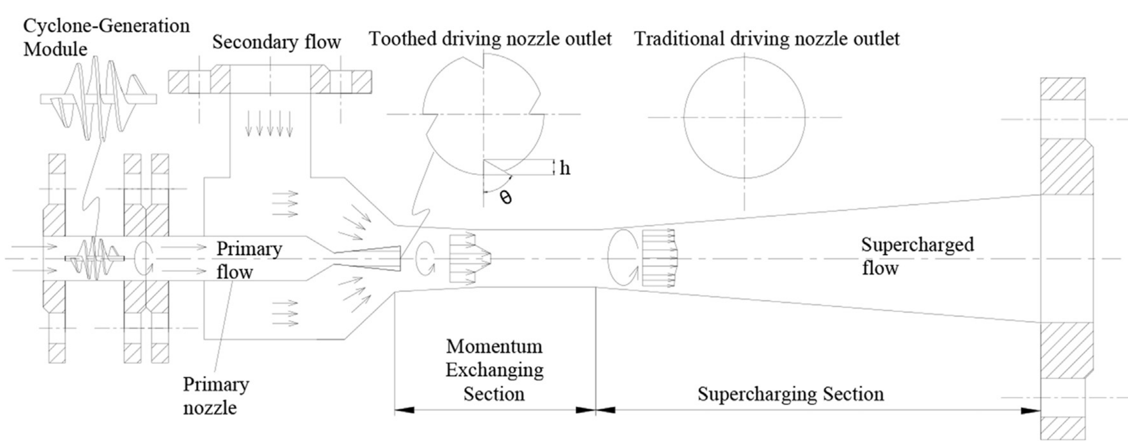

Fig. 1. Schematic diagram of ejector in different structure.

Table 1
The influences of different key sizes on *ER*s of the SCSE without cyclone generation module ($P_i = 2.7 \times 10^5$Pa, $P_s = 9.58 \times 10^3$Pa and $P_o = 2.1 \times 10^4$Pa).

Structure parameters	Sizes	m_i	m_s	ER
length of constant section in mixing chamber, L	80.0	5.18×10^{-3}	3.91×10^{-3}	0.755
	100.0	5.19×10^{-3}	4.00×10^{-3}	0.772
	120.0	5.19×10^{-3}	4.02×10^{-3}	0.774
	180.0	5.18×10^{-3}	4.01×10^{-3}	0.773
Distance between the main nozzle outlet and inlet of the mixing chamber, Lc	16.0	5.18×10^{-3}	3.94×10^{-3}	0.76
	28.0	5.19×10^{-3}	4.02×10^{-3}	0.774
	40.0	5.18×10^{-3}	4.12×10^{-3}	0.794
	66.0	5.19×10^{-3}	3.17×10^{-3}	0.61
Diverging angle,θ	3°	5.18×10^{-3}	4.01×10^{-3}	0.774
	4°	5.18×10^{-3}	4.03×10^{-3}	0.777
	6°	5.19×10^{-3}	4.02×10^{-3}	0.774
	7°	5.18×10^{-3}	3.96×10^{-3}	0.765
Radius of mixing chamber, R	9.5	5.19×10^{-3}	3.24×10^{-3}	0.623
	10.0	5.19×10^{-3}	3.71×10^{-3}	0.714
	10.3	5.19×10^{-3}	4.02×10^{-3}	0.774
	10.6	5.19×10^{-3}	3.45×10^{-3}	0.664